subcloned into the Bluescript II KS+ vector (Stratagene, La Jolla, CA), and double-strand sequenced [Sequenase Version 2.0 protocol (United States Biochemical)], after both nested-deletion (Erase-a-Base, Promega), and oligonucleotide primer-walk methodologies (primers synthesized by personnel in the D. Julius laboratory, University of California, San Francisco). The deduced amino acid sequence was initiated from the first of four potential start methionines, giving a calculated molecular size of 85,434 daltons, somewhat lower than the ~92-kD of purified β catenin. We aligned protein sequences using the Doolittle multiple alignment algorithm (*17*) and made slight refinements by eye. The GenBank (*18*) accession number for β catenin is M77013.

17. D.-F. Feng and R. F. Doolittle, *J. Mol. Evol.* **25**, 351 (1987).
18. H. S. Bilofsky and C. Burks, *Nucleic Acids Res.* **16**, 1861 (1988).
19. P. Cowin, H.-P. Kapprell, W. W. Franke, J. Tamkun, R. O. Hynes, *Cell* **46**, 1063 (1986).
20. B. Gumbiner and K. Simons, *J. Cell Biol.* **102**, 457 (1986).
21. For immunoprecipitations generated with antibody to canine E-cadherin (anti–canine E-cadherin), the negative-control antibody was a monoclonal antibody to *Xenopus* E-cadherin (anti–*Xenopus* E-cadherin) (*22*). For anti–*Xenopus* E-cadherin immunoprecipitations, the negative-control antibody was a monoclonal anti–canine E-cadherin (*20*).
22. Y. S. Choi and B. Gumbiner, *J. Cell Biol.* **108**, 2449 (1989).
23. N. J. Korman, R. W. Eyre, V. Klaus-Kovtun, J. R. Stanley, *N. Engl. J. Med.* **321**, 631 (1989).
24. P. J. Koch *et al.*, *Eur. J. Cell Biol.* **53**, 1 (1990).
25. L. Goodwin *et al.*, *Biochem. Biophys. Res. Commun.* **173**, 1224 (1990).
26. F. Rijsewijk *et al.*, *Cell* **50**, 649 (1987).
27. R. Nusse, *Trends Genet.* **4**, 291 (1988).
28. _____, A. van Ooyen, D. Cox, Y.-K. T. Fung, H. E. Varmus, *Nature* **307**, 131 (1984).
29. J. Papkoff and B. Schryver, *Mol. Cell. Biol.* **10**, 2723 (1990).
30. R. S. Bradley and A. M. C. Brown, *EMBO J.* **9**, 1569 (1990).
31. B. Riggleman, P. Schedl, E. Wieschaus, *Cell* **63**, 549 (1990).
32. M. Peifer, C. Rauskolb, M. Williams, B. Riggleman, E. Wieschaus, *Development* **111**, 1029 (1991).
33. R. O. Hynes, *Proc. Natl. Acad. Sci. U.S.A.* **70**, 3170 (1973).
34. We thank C. Blobel, G. Kimball, D. Julius, T. Brake, N. Patil, and J. Smith for advice and reagents during this project and L. Reichardt, Z. Werb, J. White, D. Aghib, and M. Peifer for comments on the manuscript. Supported by NIH Individual National Research Award 5-F32-GM-13060 (to P.M.) and by NIH award GM37432 (to B.G., who was also under the tenure of an Established Investigatorship of the American Heart Association).

7 June 1991; accepted 16 September 1991

Folding of Circularly Permuted Transfer RNAs

TAO PAN, ROBIN R. GUTELL, OLKE C. UHLENBECK*

All of the ribose-phosphate linkages in yeast tRNA^{Phe} that could be cleaved without affecting the folding of the molecule have been determined in a single experiment. Circular permutation analysis subjects circular tRNA molecules to limited alkaline hydrolysis in order to generate one random break per molecule. Correctly folded tRNAs were identified by lead cleavage at neutral pH, a well-characterized reaction that requires proper folding of tRNA^{Phe}. Surprisingly, most of the circularly permuted tRNA molecules folded correctly. This result suggests that the tRNA folding motif could occur internally within other RNA sequences, and a computer search of Genbank entries has identified many examples of such motifs.

THE TERMINI OF PROTEINS OR RNA molecules can play an important role in defining their three-dimensional structure. Although an amino acid or nucleotide sequence can fold as a motif within the polymer chain, the termini can potentially either participate in unique interactions or be needed to promote a folding pathway. One method of evaluating the importance of the termini in macromolecular folding is to study the properties of the circularly permuted isomers. A circularly permuted polymer is produced by connecting the normal termini and cleaving the backbone at another site. If such a molecule folds normally, one can conclude that the termini are unnecessary for maintaining the structure or specifying a folding pathway. However, if the circularly permuted isomer misfolds, either the correct termini are required to maintain the structure, the new termini disrupt the structure, or the folding pathway is altered. The recent demonstration that two circularly permuted isomers of *Escherichia coli* phosphoribosyl anthranilate isomerase fold normally (*1*) prompted an investigation of the folding of circularly permuted RNA molecules.

Unmodified yeast tRNA^{Phe} was chosen for study because of its well-characterized three-dimensional structure (*2, 3*). Although the biological functions of tRNA require the correct termini, it is possible to monitor the folding of tRNA^{Phe} by measuring its specific cleavage reaction with lead (*4–7*). In this reaction, a Pb^{2+} ion is bound to the nucleotide bases U59 and C60 in the T loop and promotes a specific cleavage between U17 and G18 in the D loop. An analysis of the Pb^{2+} cleavage rates of more than 50 yeast tRNA^{Phe} mutants reveals that the rate of cleavage is very sensitive to the folded structure (*7*). Single mutations that disrupt tertiary interactions as far away as 16 to 20 Å from the lead binding site show a 3- to 20-fold reduction in the cleavage rate. The cleavage rate is restored when compensatory mutations allow the formation of an alternate tertiary interaction (*7*). The cleavage rate is not affected by mutations not expected to alter the folding of tRNA^{Phe} (*7*). Thus, this reaction is useful for examining the folding of circularly permuted tRNA molecules.

Circular permutation analysis (CPA) was carried out to determine which of the 76 possible circularly permuted tRNA^{Phe} molecules fold correctly (Fig. 1). The G1A mutant of tRNA^{Phe} was used because it has a mismatched terminal base pair that permits efficient formation of a circular tRNA by T4 RNA ligase (*8*) without affecting its ability to cleave with lead. The starting material for CPA was prepared by cleaving the circular tRNA with lead, introducing a ^{32}P label at the lead cleavage site between U17 and G18, and religating the tRNA (Fig. 1A). The uniquely labeled circular tRNA molecules were subjected to limited alkaline hydrolysis under denaturing conditions such that each molecule was cleaved no more than once and all bonds were cut with approximately equal frequency. The resulting collection of 76 different circularly permuted tRNAs was renatured and then treated with lead in the presence of Mg^{2+}. Those molecules that folded correctly, and therefore were cleaved with lead, produced an oligonucleotide with a 3′ ^{32}P label at the ribose of U17 and a 5′ terminus at the site generated by alkaline hydrolysis (Fig. 1B). For circularly permuted tRNAs that did not cleave with lead, no such shorter ^{32}P-labeled oligonucleotide was formed. Thus, separation of the reaction products on a sequencing gel and subsequent autoradiography identified all of the folding-permissive backbone breaks.

A typical CPA experiment is shown in Fig. 2A. The conditions chosen for alkaline hydrolysis resulted in a nearly uniform population of breaks when end-labeled linear tRNA was hydrolyzed. It is striking to find that a large number of circularly permuted tRNAs still cleaved with lead. We quantitated the radioactivity in each band and compared it to the band corresponding to the normal tRNA (break at ribose phosphate 1) to estimate the relative extent of lead cleavage at each position. Circularly permuted tRNAs with 5′ termini at 54 of 68 analyzable backbone positions had comparable or greater extents of lead cleavage than the native tRNA (Fig. 3). These positions include virtually the entire acceptor and T stems as well as most of the anticodon stem

T. Pan and O. C. Uhlenbeck, Department of Chemistry and Biochemistry, University of Colorado, Boulder, CO 80309.
R. R. Gutell, Department of Molecular and Cellular Developmental Biology, University of Colorado, Boulder, CO 80309.

*To whom correspondence should be addressed.

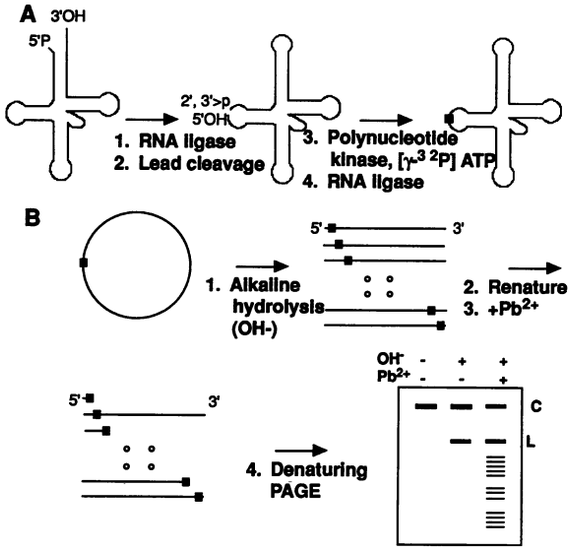

Fig. 1. Schematic representation of the circular permutation analysis (CPA). (**A**) Introduction of a unique label at the lead cleavage site. (**B**) CPA. The cloverleaf form of tRNA in (A) is shown as a circle in (B). Solid squares indicate the position of the unique ^{32}P label. C and L correspond to circular and linear tRNA, respectively.

and loop. Interestingly, lead cleavage is strongly enhanced (up to sevenfold) in several circularly permuted tRNAs with breaks in the anticodon loop. This result confirms an earlier report of increased lead cleavage of yeast $tRNA^{Phe}$ missing Y37 (*5*) and supports the notion that changes in the anticodon conformation can alter the structure (*9*) or dynamics at a spatially distant site.

All 14 circularly permuted tRNAs not cleaved with lead had termini located in the central core of the tRNA (Fig. 3). Most of these positions are directly involved in tertiary base pairing, including the highly structured G53 to G57 region in the T loop and the U8 to A14 region in the D stem. Although it is tempting to speculate that these highly constrained regions of the molecule are more sensitive to chain breakage, it is striking that a number of other sites in the tRNA core can serve as termini for circularly permuted tRNAs. These include all of the ribose phosphates in the variable loop and the 3′ half of the T loop, including the ribose phosphates 59 and 60 whose nucleotide bases actually bind the lead ion. Thus, no simple interpretation can be given to explain which termini permit correctly folded circularly permuted tRNAs.

We also performed CPA under several different buffer conditions known to affect RNA folding. Varying the Mg^{2+} concentration between 3 and 15 mM (Fig. 2A) or addition of 1.5 mM spermine (Fig. 2B) at 7.5 mM Mg^{2+} did not significantly alter the pattern of bands, even though the intrinsic rate of lead cleavage was changed. Similar results were observed when CPA was performed at 37°C. However, in the presence of 1.5 M urea or formamide, the extent of lead cleavage of tRNAs with breaks at the ends of the acceptor helix (ribose phosphate 67) and T helix (ribose phosphates 66 and 50) were significantly decreased (Fig. 2B and Table 1). Higher concentrations of urea or formamide led to destabilization of additional circularly permuted tRNAs having backbone breaks within the T loop (ribose phosphates 61, 60, 59, and 58; see Table 1). These results are consistent with the notion that certain positions are more important to the folding of tRNA and thus more sensitive to disruption by RNA denaturants. However, addition of 15% ethanol apparently induced stabilization of the breaks within T loop riboses, including the critical U-turn consisting of U54 to G57 (Table 1). This stabilization effect by ethanol may be coupled to transitions of helical conformation as observed for DNA helices (*10*). The CPA results performed under varying buffer conditions strongly suggest that decreasing extents of lead cleavage are mostly due to defects in folding, not to a decrease of lead binding.

Our experiments indicate that relocation of termini of tRNA can often be accomplished without alteration of the basic folding geometry. Since most of the new termini are on the surface of the tRNA structure (Fig. 3B), the chains could be extended in both 3′ and 5′ directions. Thus, tRNA-like folding motifs may exist internally within the sequences of other RNA molecules. The potential presence of such motifs in GenBank was examined with the program RNAMOT (*11*), which allows the user to define combinations of sequence and secondary structural elements. In our search, the five most highly conserved tertiary interactions within the tRNA core were required. Since both the acceptor stem and anticodon hairpin are not part of the central core and can be reduced to three or fewer base pairs without affecting lead cleavage (*12*), these regions were allowed to vary. In addition, the number of nucleotides in the α region (residues 16 and 17) were permitted to vary from 1 to 20 nucleotides, based upon a range of lengths observed in natural tRNAs and the existence of a synthetic $tRNA^{Phe}$ variant with 12 extra nucleotides that cleave with lead normally (*12*).

Searches for circularly permuted tRNA-like folding motifs were performed with termini at the folding-permissive positions

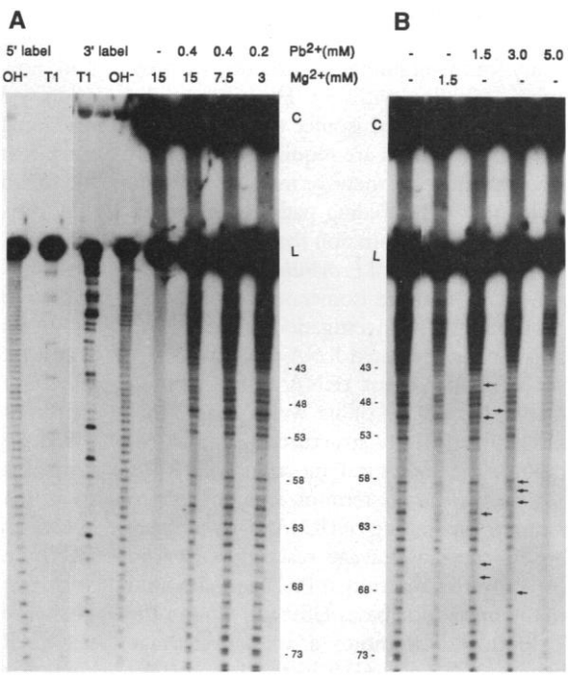

Fig. 2. CPA of yeast $tRNA^{Phe}$ (*19*) analyzed on 10% denaturing polyacrylamide gels. Alkaline hydrolysis of circular $tRNA^{Phe}$ (C) yields a mixture of circularly permuted linear (L) tRNA molecules. Lead cleavage of this mixture at (**A**) varying Mg^{2+} and Pb^{2+} concentrations and (**B**) in 0.4 mM Pb^{2+} and 7.5 mM Mg^{2+} for varying spermine (bottom row, mM) or urea (top row, M) concentrations reveals cleavage products for those circularly permuted tRNA molecules that fold correctly. All reactions were performed in 5.5 mM MOPS, pH 7.0. The size of these products can be determined by comparing to the alkaline hydrolysis product (OH^-) and ribonuclease T1 digestion (T1) of linear tRNA that is 5′ or 3′ ^{32}P-labeled at the lead cleavage site. The numbers parallel to the bands correspond to ribose phosphate positions that have been disrupted by alkaline hydrolysis prior to lead cleavage. The horizontal arrows in (B) indicate the bands that either show significantly decreased (pointing to left) or increased (pointing to right) lead cleavage extents.

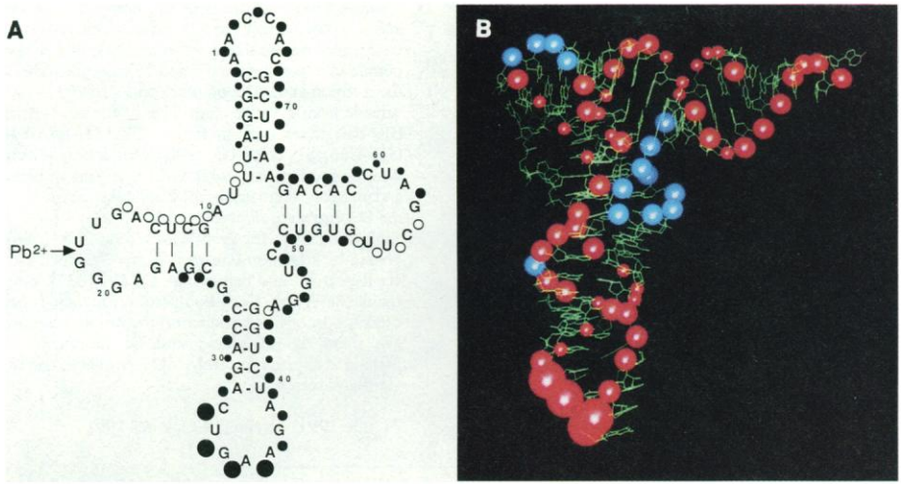

Fig. 3. Summary of CPA in 5.5 mM MOPS, pH 7.0, 7.5 mM Mg^{2+}, and 0.4 mM Pb^{2+}. Yeast $tRNA^{Phe}$ was presented either in its secondary (**A**) or tertiary (**B**) structure. The solid circles (A) or red spheres (B) represent positions where the ribose phosphate can be disrupted and the resulting circularly permuted tRNAs are correctly folded. The open circles (A) or blue spheres (B) indicate positions where the backbone breaks reduce the extent of lead cleavage by more than fivefold. If no circle or sphere is shown, the corresponding ribose phosphate positions could not be analyzed because of the resolution of the gel electrophoresis. The size of the solid circles (A) or red spheres (B) represent the ratios of the lead cleavage relative to that of the standard tRNA (break at ribose phosphate 1): (•), 0.3 to 0.8; (●), 0.8 to 3.0; and (●), 3.0 to 7.0. The ribose positions 15 to 1 and 76 to 74 were analyzed on 20% denaturing gels.

Table 1. CPA of yeast $tRNA^{Phe}$ in the presence of denaturants.

Denaturant	Ribose phosphate positions where lead cleavage rate:	
	Increases	Decreases
Urea (1.5 M)	41	67, 66, 61, 50, 45
Urea (3.0 M)	49	68, 67, 66, 61, 60 59, 58, 50, 45
Formamide (15%)		67, 66, 45
Formamide (30%)		67, 66, 61, 60, 59, 50, 45
Ethanol (15%)	60, 59, 56, 55, 54	

27, 48, and 58 (Fig. 4B). In the ~55 million nucleotides in GenBank 67.0, a number of such motifs (20, 21, and 105, respectively) were found in the sense strands of known genes. Four examples of such motifs are shown in Fig. 4, C to F. In each case, the presence of one or more potential base triples that were not included in the search reinforces the notion that these RNAs fold like tRNA.

Why might tRNA-like folding motifs exist in other RNA molecules? One possibility is that, like the hairpin or the pseudoknot, the tRNA motif is simply an efficient means of folding RNAs into a compact tertiary structure. In addition, tRNA-like motifs can potentially interact with one of the many tRNA binding proteins present in the cytoplasm at high concentrations. Indeed, the ability of some bacterial tRNA synthetases to bind to a tRNA-like structure in their own mRNA and repress translation is well documented (*13*). The tRNA motifs found in the coding sequence of the *E. coli* tufA and *Caenorhabditis elegans* myo-3 gene (Fig. 4, D and E) may have a similar regulatory function. Binding proteins for tRNA may interact with the motif in the 3′ untranslated region of the mouse BCL-2 gene (Fig. 4C) and affect processing or mRNA stability. The tRNA-like structure in the influenza virus (Fig. 4F) may be required for infection as has previously been demonstrated for tRNA-like structure at the 3′ terminus of many plant viral genomes (*14*).

It is likely that many of the backbone breaks that allow proper folding of circularly permuted tRNA may also permit correct folding in standard tRNA. Lead cleavage of $tRNA^{Phe}$ cleaved at ribose phosphate 37 has been previously reported (*5, 15*). Another construct that consists of two fragments comprised of nucleotides 1 to 48 and 47 to 76 and that is analogous to a circularly permuted tRNA with a break at ribose phosphate 47 also shows a normal rate of lead cleavage (*12*). The propensity for RNA molecules to maintain structure and activity in the presence of backbone breaks has been noted (*16*) and was exploited to convert autocatalytic RNAs into RNA enzymes that exhibit multiple turnovers (*17, 18*). If a selection procedure is available, CPA can be used with other RNAs to systematically locate ribose backbone positions where the phosphodiester bond can be disrupted without affecting folding. We expect that, as with $tRNA^{Phe}$, other RNAs may often have a high enough local energy of folding to compensate for chain cleavage so that many folding permissive backbone breaks would be found.

Many RNA molecules have their 5′ and 3′ termini in close proximity because of the presence of complementary sequences that result in helix formation. Perhaps circular

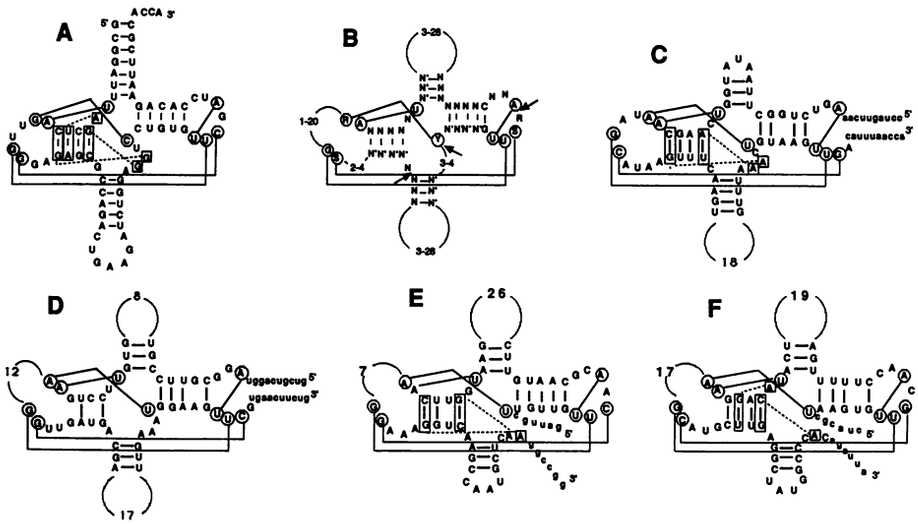

Fig. 4. Examples of circularly permuted tRNA-like motifs in the GenBank version 67.0. (**A**) Yeast $tRNA^{Phe}$. (**B**) Schematic presentation of the descriptor (*22*) (N, any nucleotide; R, A or G; Y, C or T; and S, C or G). The arrows indicate the 5′ termini (ribose phosphate 27, 48, and 58) of the circularly permuted tRNAs in the search. (**C**) Mouse BCL-2 gene, 3′ untranslated region [nucleotides (nt) 7513 to 7610]. (**D**) *Escherichia coli* tufA gene (nt 507 to 613). (**E**) *Caenorhabditis elegans* myo-3 gene, exon 6 (nt 6789 to 6888). (**F**) Influenza PB1 polymerase gene (nt 2081 to 2183). The five tertiary base-base interactions retained in our search are connected by solid lines. The potential base triples are boxed and connected by dashed lines. The numbers embedded in semicircles indicate the actual number of nucleotides found in the loops that were variable in our search program.

permutation may have played a role in the evolution of these RNAs. Some RNA folding motifs may have evolved with very different termini prior to a rare event where a circular RNA intermediate is formed and cleaved at a different location to result in circularly permuted RNA. Subsequent reverse transcription could convert the circularly permuted motif back into DNA. Such events may explain the appearance of circularly permuted tRNA-like motifs in other RNAs or may suggest that tRNA itself originally appeared as a circularly permuted isomer.

REFERENCES AND NOTES

1. K. Luger, U. Hommel, M. Herold, J. Hofsteense, K. Kirschner, *Science* **243**, 206 (1989).
2. G. J. Quigley and A. Rich, *ibid.* **194**, 796 (1976).
3. S.-H. Kim, in *Transfer RNA*, S. Altman, Ed. (MIT Press, Cambridge, MA, 1978), pp. 248–293.
4. C. Werner *et al.*, *Biochim. Biophys. Acta* **432**, 161 (1976).
5. W. J. Krzyzosiak *et al.*, *Biochemistry* **27**, 5771 (1988).
6. R. S. Brown *et al.*, *ibid.* **24**, 4785 (1985).
7. L. S. Behlen *et al.*, *ibid.* **29**, 2515 (1990); L. S. Behlen and O. C. Uhlenbeck, unpublished results.
8. A. G. Bruce and O. C. Uhlenbeck, *Nucleic Acids Res.* **5**, 3665 (1978).
9. E. Westhof *et al.*, *J. Mol. Biol.* **184**, 119 (1985).
10. V. I. Ivanov *et al.*, *Biopolymers* **12**, 89 (1973); W. Saenger, *Principles of Nucleic Acid Structure* (Springer-Verlag, New York, 1984), pp. 368–384.
11. D. Gautheret *et al.*, *Cabios* **6**, 325 (1990).
12. T. Pan, A. DiRenzo, O. C. Uhlenbeck, unpublished results.
13. M. Springer *et al.*, *EMBO J.* **8**, 2417 (1989); F. Dardel *et al.*, *Mol. Gen. Genet.* **223**, 121 (1990).
14. T. W. Dreher and T. C. Hall, *J. Mol. Biol.* **201**, 31 (1988); T. W. Dreher *et al.*, *ibid.* **206**, 425 (1989).
15. J. R. Sampson *et al.*, *Cold Spring Harbor Symp. Quant. Biol.* **52**, 267 (1987).
16. M. W. Gray and M. N. Schnare, in *The Ribosome: Structure, Function and Evolution*, W. Hill *et al.*, Eds. (American Society for Microbiology, Washington, DC, 1990), pp. 589–597.
17. O. C. Uhlenbeck, *Nature* **328**, 596 (1987).
18. A. J. Zaug and T. R. Cech, *Science* **231**, 470 (1986).
19. A DNA plasmid encoding a G1A mutant of YF0 was transcribed by T7 RNA polymerase and purified as previously described (*20, 21*), except that a fivefold excess of adenosine 5′-monophosphate over adenosine triphosphate (ATP) was included in the transcription reaction to generate RNA with a 5′-monophosphate. In order to form an intramolecular circle, 10 μM linear tRNA was incubated in 50 mM tris, pH 7.6, 10 mM $MgCl_2$, 10 mM β-mercaptoethanol, 0.2 mM ATP, bovine serum albumin, (0.1 mg/ml) 15% dimethyl sulfoxide, and T4 RNA ligase (1 U/μl) for 2 hours at 37°C. In order to introduce a unique ^{32}P label at the Pb^{2+} cleavage site, 2 μM circular tRNA was cleaved in 15 mM MOPS, pH 7.0, 15 mM $MgCl_2$, and 0.4 mM lead acetate at 23°C for 6 min followed by ethanol precipitation to remove Pb^{2+}. The precipitated tRNA was then redissolved to 3.5 μM in 30 mM tris, pH 8.0, 15 mM $MgCl_2$, and T4 polynucleotide kinase (1.5 U/μl) and incubated for 45 min at 37°C. Upon addition of 30 mM tris, pH 7.5, 8 mM dithiothreitol, and [γ-^{32}P]ATP, the reaction mixture was further incubated at 37°C for another 30 min. The resulting tRNA with a ^{32}P label at its 5′ end and free 3′-OH, was then religated under conditions described above. Alkaline hydrolysis was carried out with 7 μM circular tRNA in 1 mM glycine, 0.4 mM $MgSO_4$, pH 9.5, by boiling for 45 s. The tRNA was renatured in 30 mM MOPS, pH 7.0, by heating for 2 min at 85°C. Lead cleavage was finally carried out under conditions as described in legend to Fig. 2 for 6 min at 23°C. The cleavage reaction was stopped by addition of an equal volume of 8 M urea and 50 mM EDTA, and the reaction mixture was then directly loaded onto a 10 or 20% polyacrylamide gel that contained 7 M urea. To ensure that no new Pb^{2+} cleavage site is generated upon circular permutation, it was necessary to show that all of the fragments shorter than full-length linear tRNA contained a 3′-terminal ^{32}P phosphate. This was done by incubating an aliquot of the lead-cleaved reaction mixture in 0.1 M HCl for 1 hour at 25°C to hydrolyze the 2′,3′-cyclic terminal phosphate, followed by neutralization with NaOH and treatment with 1 U of calf intestine alkaline phosphatase in 50 mM tris, pH 8.0, at 37°C for 1 hour. When the reaction mixture was analyzed by denaturing polyacrylamide gel electrophoresis, no radioactive bands other than the circular and full-length linear tRNAs were detected, showing that the 3′ ^{32}P was removed from all of the fragments.
20. J. F. Milligan and O. C. Uhlenbeck, *Methods Enzymol.* **180**, 51 (1989).
21. J. R. Sampson and O. C. Uhlenbeck, *Proc. Natl. Acad. Sci. U.S.A.* **85**, 1033 (1988).
22. Descriptor of the GenBank search: Both the anti-codon and acceptor stems were reduced to a minimum of 3 base pairs, and the acceptor and anticodon loops were permitted to vary between 3 and 28 bases; in addition, the α region in the D loop (nucleotides 16 and 17) was variable from 1 to 20 bases. Five of the nine tertiary base-base interactions in tRNA, U8-A14, R15-Y48, G18-U55, S19-S56 (G/C19-C/G56), and U54-A58, were retained in our search. G-U base pairs in helices and up to one mismatch in the T and two mismatches in the D stems were allowed.

23. Supported by NIH grant GM37552. T.P. is supported by a Damon Runyon–Walter Winchell Cancer Research Fund Fellowship, DRG-1103. We also thank the W. M. Keck Foundation for their generous support of RNA science on the Boulder campus. We thank D. Gautheret and R. Cedergren for making the program RNAMOT available for our GenBank search.

31 July 1991; accepted 4 October 1991

Viviparous Leaves Produced by Somatic Activation of an Inactive Cytokinin-Synthesizing Gene

JUAN JOSÈ ESTRUCH, ELS PRINSEN, HARRY VAN ONCKELEN, JEFF SCHELL, ANGELO SPENA*

Tobacco plants that are somatic mosaics for expression of a cytokinin-synthesizing gene have viviparous leaves. Such a formation of shoots in an abnormal position represents a significant deviation from the usual organization of the plant body where a central axis produces shoots only in the axils of lateral leaf appendages and according to a precise phyllotactic pattern. This report links vivipary to the expression of a gene whose product is involved in the synthesis of the phytohormone cytokinin.

UNDER NATURAL PLANT GROWTH conditions, leaves that form adventitious buds on their surfaces or edges are said to be viviparous (*1, 2*). Depending on the plant species, this manifestation of totipotency of differentiated leaf cells is a phenomenon occurring either as part of a normal developmental process (*3, 4*) or as a teratological event (*1*). Knowledge of the underlying cellular mechanisms is scant. We report here that vivipary is acquired by tobacco leaves that are somatic genetic mosaics for the expression of a cytokinin-synthesizing gene.

In culture with added growth regulators, leaf explants of several species express new developmental patterns (*5*). In particular, cytokinins are routinely used to regenerate plants from explants (*5*). Expression of cytokinin in vivo was altered here with the use of the crown gall *ipt* gene. Crown galls are neoplastic plant tissues resulting from the transfer and expression of oncogenes carried on a transferable DNA segment (T-DNA) of the Ti plasmid of the bacterial pathogen *Agrobacterium tumefaciens*. One of these oncogenes, *ipt*, codes for an isopentenyltransferase, which is involved in cytokinin synthesis (*6*). Expression of the *ipt* gene under the control of the 35*S* RNA promoter from cauliflower mosaic virus (CaMV) increases the cytokinin content up to 137 times in transgenic shoots of *Nicotiana tabacum, N. rustica*, and *N. plumbaginifolia* (*7*). These shoots exhibit loss of apical dominance and are unable to root (*7, 8*). The *ipt* gene under control of inducible (*9–11*) or tissue-specific promoters (*12*) circumvents the inhibitory effect of high endogenous levels of cytokinin on root formation. However, most inducible promoters have a low basal level of constitutive expression, and tissue-specific promoters have localized expression occurring only after differentiation, limiting the study of the influence of cytokinins on plant development.

We have inserted the maize transposon *Ac* (*13–16*), into the untranslated leader sequence of the 35*S-ipt* gene to inactivate the *ipt* gene (Fig. 1). Somatic transposon excision subsequently reactivates expression of the 35*S-ipt* gene. Whereas early excision events are expected to generate teratoma-like tissues unable to form roots, excision events taking place late in plant development

J. J. Estruch, J. Schell, A. Spena, MPI für Züchtungsforschung, Carl-von-Linne weg, 10, 5000 Köln 30, Germany. E. Prinsen and H. Van Onckelen, UIA, Universiteitsplein, B-2610 Antwerpen (Wilrijk), Belgium.

*To whom correspondence should be addressed.